Preparation, Characterization, and Luminescence Properties of Gallium−Metal Face-to-Face Diporphyrins (M = H_2, GaL, Ru(CO)(OH), Co)

Pierre D. Harvey,* Nathalie Proulx, Geneviève Martin, and Marc Drouin

Département de Chimie, Université de Sherbrooke, Sherbrooke, P. Q. Canada J1K 2R1

Daniel J. Nurco and Kevin M. Smith*

Department of Chemistry, University of California, Davis, California 95616

Frédéric Bolze,† Claude P. Gros, and Roger Guilard*

Laboratoire d'Ingénierie Moléculaire pour la Séparation et les Applications des Gaz (L.I.M.S.A.G.), U.M.R. 5633, Faculté des Sciences "Gabriel", 6, boulevard Gabriel, 21000 Dijon, France

Received December 27, 2000

The preparation and characterization of a new series of mixed metal cofacial anthracene-bridged diporphyrins (DPA) containing a GaL fragment (L = OMe, OH) and another metallic center (M = GaL, Ru(CO)(OH), Co, and H_2 (i.e. free base)) are reported. The luminescence properties at 298 and 77 K, in degassed EtOH solution, are also reported, and are characterized by a weak $\pi\pi^*$ fluorescence ($2 < \tau_F < 7$ ns) arising from the low energy Q-bands ($S_1 \rightarrow S_0$). In the mixed diporphyrin systems, a strong $\pi\pi^*$ fluorescence is detected from the free base, while the transition metalloporphyrins of Co(II) and Ru(II) do not emit. The homobimetallic di[Ga(OMe)] species exhibits an unprecedented double $\pi\pi^*$ fluorescence arising from the two lowest energy absorption Q-bands. On the basis of a comparison with photophysical data on GaL monoporphyrins, the weak fluorescence and absence of phosphorescence for most cases indicate efficient intramolecular quenching. To define structural features, the X-ray structures of (DPA)[Ga(OMe)]$_2$ (**2**), (DPA)[Ga−(OH)−Ru(CO)] (**5a**), and (DPA)[Ga(OMe)−Ru(MeOH)-(CO)] (**5b**) have been obtained. The structures of **5a** and **5b** demonstrate an interesting aspect of the structural chemistry of these ligands related to the internal methoxide and methanolic ligands in **5b** (resulting in a large interplanar separation and center-to-center distance) and the internal metal-bridging hydroxyl ligand in **5a** (resulting in a small interplanar separation and center-to-center distance). These data support previously reported discussions on the ability of the DPA and the DPB analogue (diporphyrinylbiphenylenyl) ligands to open and close their "bite" around the binding pocket between the porphyrin macrocycles.

Introduction

The preparation and investigations of homobimetallic cofacial diporphyrins have attracted significant attention over the past 15 years or so, particularly for the dicobalt(II) and diruthenium(II) species in relation with their applications for the reduction of dioxygen[1−7] and dinitrogen[8] and the activation of dihydrogen.[9] More recently, the preparation of heterobimetallic cofacial diporphyrins complexes has been made,[10,11] and of particular interest, a series of Al−Co complexes have been reported.[10] In these cases the Al center is selected for its Lewis acid properties, while the Co(II) ion is used to bind O_2. Although the electrocatalytical behavior of the cofacial diporphyrin species has been fully investigated,[1−6] the photocatalytical and photophysical properties have not been explored so far, except for resonance Raman studies on the dicobalt(II) and its O_2 adduct and diruthenium(II) complexes.[12,13] Literature shows that metalloporphyrins exhibit rich photoredox[14−17] and luminescence properties,[18−21] and investigations of multiporphyrin assemblies

* To whom correspondence should be sent.

† Also affiliated with Université de Sherbrooke.

(1) Collman, J. P.; Hutchison, J. E.; Lopez, M. A.; Tabard, A.; Guilard, R.; Seok, W. K.; Ibers, J. A.; L'Her, M. *J. Am. Chem. Soc.* **1992**, *114*, 9869−9877.
(2) Durand, R. R., Jr.; Bencosme, C. S.; Collman, J. P.; Anson, F. C. *J. Am. Chem. Soc.* **1983**, *105*, 2710−2718.
(3) Le Mest, Y.; Inisan, C.; Laouenan, A.; L'Her, M.; Talarmin, J.; El Kalifa, M.; Saillard, J.-Y. *J. Am. Chem. Soc.* **1997**, *119*, 6095−6106.
(4) Chang, C. K.; Liu, H.-Y.; Abdalmuhdi, I. *J. Am. Chem. Soc.* **1984**, *106*, 2725−2726.
(5) Durand, R. R., Jr.; Collman, J. P.; Anson, F. C. *J. Electroanal. Chem.* **1983**, *151*, 289−294.
(6) Liu, H.-Y.; Abdalmuhdi, I.; Chang, C. K.; Anson, F. C. *J. Phys. Chem.* **1985**, *89*, 665−670.
(7) Guilard, R.; Brandès, S.; Tardieux, C.; Tabard, A.; L'Her, M.; Miry, C.; Gouerec, P.; Knop, Y.; Collman, J. P. *J. Am. Chem. Soc.* **1995**, *117*, 11721−11729.
(8) Collman, J. P.; Hutchison, J. E.; Lopez, M. A.; Guilard, R.; Reed, R. A. *J. Am. Chem. Soc.* **1991**, *113*, 2794−2796.
(9) Collman, J. P.; Hutchison, J. E.; Wagenknecht, P. S.; Lewis, N. S.; Lopez, M. A.; Guilard, R. *J. Am. Chem. Soc.* **1990**, *112*, 8206−8208.
(10) Guilard, R.; Lopez, M. A.; Tabard, A.; Richard, P.; Lecomte, C.; Brandès, S.; Hutchison, J. E.; Collman, J. P. *J. Am. Chem. Soc.* **1992**, *114*, 9877−9889.
(11) Guilard, R.; Brandès, S.; Tabard, A.; Bouhmaida, N.; Lecomte, C.; Richard, P.; Latour, J. M. *J. Am. Chem. Soc.* **1994**, *116*, 10202−10211.
(12) Kim, D.; Su, Y. O.; Spiro, T. G. *Inorg. Chem.* **1986**, *25*, 3993−3997.
(13) Proniewicz, L. M.; Odo, J.; Goral, J.; Chang, C. K.; Nakamoto, K. *J. Am. Chem. Soc.* **1989**, *111*, 2105−2110.
(14) Leland, B. A.; Joran, A. D.; Felker, P. M.; Hopfield, J. J.; Zewail, A. H.; Dewan, P. B. *J. Phys. Chem.* **1985**, *89*, 5571−5573 and references therein.

10.1021/ic001446j CCC: $20.00
Published on Web 07/20/2001

have also recently appeared.[22,23] Gallium porphyrins are known to be good emitters[24,25] and can also be used as Lewis acids as well, hence taking advantage of an inherent spectroscopic probe. We now wish to report the preparation of a series of new heterobimetallic cofacial diporphyrins, all containing Ga(III) centers and using the anthracenyl spacer (referred as DPA in this paper). The luminescence properties are also reported.

Experimental Section

Chemicals. The synthesis and handling of each complex was carried out under an argon atmosphere employing Schlenck techniques. All chemicals were of reagent grade quality. Merck type 60 (230−400 mesh) silica gel and Merck type 90 (70−230 mesh, activity II−III) aluminum oxide were used for column chromatography.

Synthesis of H_4(DPA) (1). The free base **1** was prepared as described in the literature.[4,10,26−28]

Synthesis of (DPA)[Ga(OMe)]$_2$ (2). Under an argon atmosphere, 0.72 mmol of $GaCl_3$ (2.50 mL of a 5% solution in glacial acetic acid) was added to a solution of 0.13 mmol (150 mg) of H_4(DPA) (**1**) and 1.22 mmol (100 mg) of anhydrous sodium acetate in 40 mL of dry, degassed benzonitrile. The mixture was refluxed for 90 min during which the progress of the metalation reaction was monitored by UV−vis spectroscopy. The solvent was removed under vacuum, and the residue was then dissolved in methylene chloride (50 mL). The organic phase was washed thoroughly with water then dried with magnesium sulfate. Chromatography on basic alumina (4 × 25 cm column) eluted with methylene chloride/methanol (gradually from 99.5/0.5 to 98.5/1.5) followed by crystallization with methylene chloride/heptane (50/50) afforded the title compound (**2**) (140 mg, 80%) as purple crystals. Anal. Calcd for (DPA)[Ga(OMe)]$_2$: C, 72.30; H, 6.37; N, 8.43. Found: C, 72.59; H, 6.61; N, 8.45. ^{1}H NMR (C_6D_6): 9.48 (s, 2H, meso); 9.20 (s, 4H, meso); 9.22 (s, 1H, 10-anth.); 8.56 (s, 1H, 9-anth.); 8.23 (d, 2H, anth.); 6.78 (m, 2H, anth.); 6.75 (m, 2H, anth.); 4.46 (m, 8H, Et); 3.98 (m, 8H, Et); 3.39 (s, 12H, Me); 1.90 (s, 12H, Me); 1.71 (m, 12H, Et); 1.48 (m, 12H, Et); −2.25 (s, 6H, OCH_3). MS SIMS (NBA): *m*/*z* 1267 [M − 2MeO + 1]$^+$; 1418 [M − 2MeO + NBA]$^+$. UV−vis (CH_2Cl_2) λ_{max} nm (ϵ 10^{-3} M^{-1} cm^{-1}): 388 (340); 543 (16); 573 (13). IR (KBr) ν cm^{-1}: 2964, 2929, 2870 (CH).

Synthesis of H_2(DPA)Zn (3). The synthesis of (**3**) followed the procedure of Collman et al. for the DPB (diporphyrinylbiphenylenyl) analogues.[26,29] During the purification by column chromatography, the product band was eluted with methylene chloride/methanol (gradually from 98/2 to 96/4). UV−vis (benzene) λ_{max} nm (ϵ.10^{-3} M^{-1} cm^{-1}): 399 (196.6); 507 (7.0); 539 (10.5); 575 (11.6); 630 (1.3). IR (CsI) ν cm^{-1}: 3278 cm^{-1} (NH).

Synthesis of H_2(DPA)[Ga(OMe)] (4a). Under an argon atmosphere, 0.43 mmol of $GaCl_3$ (1.50 mL of a 5% solution in acetic acid) was added to a solution of 0.35 mmol (417 mg) of H_2(DPA)Zn (**3**) and 1.0 mmol (82 mg) of anhydrous sodium acetate in 35 mL of dry and deareted benzonitrile. The mixture was heated to 180 °C for 90 min during which the progress of the metalation reaction was monitored by UV−vis spectroscopy. The solvent was removed under vacuum, and the residue was then dissolved in methylene chloride (200 mL). Hydrochloric acid (6 M, 50 mL) was added, and the mixture was stirred vigorously for 30 min. The solution was neutralized with 10% sodium hydrogenocarbonate, and the resulting mixture was stirred for 15 min. The organic phase was separated, washed sequentially with water and brine, then dried over magnesium sulfate. Chromatography on basic alumina (5 × 25 cm column) eluted with methylene chloride/methanol (96/4) followed by crystallization with methylene chloride/methanol (50/50) afforded the title compound (**4a**) (140 mg, 32% yield) as purple crystals. Anal. Calcd for H_2(DPA)[Ga(OMe)]: C, 77.16; H, 6.80; N, 9.11. Found: C, 77.48; H, 6.93; N, 9.21. ^{1}H NMR (C_6D_6): 9.63 (s, 1H, meso); 9.44 (s, 1H, meso); 8.93 (s, 1H, 10-anth.); 8.89 (s, 2H, meso); 8.77 (s, 1H, 9-anth.); 8.74 (s, 2H, meso); [8.67−8.65 (m, 2H); 8.28 (m, 2H); 8.25 (m, 2H)] anth.; 3.99 (m, 4H, Et); 3.77 (m, 4H, Et); 3.31 (m, 8H, Et); 2.95 (s, 12H, Me); 2.00 (s, 6H, Me); 1.98 (s, 6H, Me); 1.70 (m, 12H, Et); 1.29 (m, 12H, Et); −1.68 (s, 3H, OCH_3); −4.80 (s, 1H, NH); −5.11 (s, 1H, NH). MS SIMS (NBA): *m*/*z* 1198 [M − MeO]$^+$; 1352 [M − MeO + NBA + 1]$^+$. UV−vis (CH_2Cl_2) λ_{max} nm (ϵ 10^{-3} M^{-1} cm^{-1}): 394 (306); 507 (14); 541 (19); 579 (17); 628 (3). IR (KBr) ν cm^{-1}: 3251 (NH); 2962, 2928, 2869 (CH).

Synthesis of (DPA)[Ga−(OH)−Ru(CO)] (5a). Under an argon atmosphere, 0.08 mmol of $Ru_3(CO)_{12}$ (40 mg) was added to a solution of 0.04 mmol (50 mg) of H_2(DPA)[Ga(OMe)] (**4a**) in 20 mL of deareted 2-methoxyethanol. The mixture was then refluxed for 3 h 30 min, the progress of the metalation reaction being monitored by UV−vis spectroscopy. The solvent was then removed under vacuum. The residue obtained was first chromatographed on basic alumina (4 × 20 cm column) eluted with toluene/methanol (gradually from 100/0 to 95/5) then on silica (3 × 15 cm column) eluted with diethyl ether. Evaporation of the solvent afforded the title compound (**5a**) (20 mg, 36%) as a purple powder. Anal. Calcd for (DPA)[Ga−(OH)−Ru(CO)]: C, 70.64; H, 5.93; N, 8.34. Found: C, 70.59; H, 6.65; N, 7.26. ^{1}H NMR (C_6D_6): 9.47 (s, 1H, meso); 9.20 (s, 2H, meso); 8.89 (s, 1H, meso); 8.83 (s, 1H, 10-anth.); 8.65 (s, 2H, meso); 8.48 (d, 1H, 2-anth.); 8.43 (d, 1H, 7-anth.); 7. 96 (d, 1H, 4-anth.); 7.86 (d, 1H, 5-anth.); 7.77 (s, 1H, 9-anth.); 7.74 (m, 2H, 3-anth., 6 anth.); 4.53 (m, 4H, Et); 4.38 (m, 4H, Et); 4.18 (m, 4H, Et); 3.95 (m, 4H, Et); 3.65 (m, 6H, Me); 3.47 (s, 6H, Me); 1.96 (s, 6H, Me); 1.82 (t, 6H, Me); 1.76 (s, 6H, Me); 1.72 (t, 6H, Et); 1.65 (s, 6H, Me); 1.55 (m, 6H, Et); −15.87 (s, 1H, μ-OH). MS MALDI-TOF: 1297 [M − CO − OH]$^{+\cdot}$, 1314 [M − CO]$^{+\cdot}$, 1325 [M − OH]$^{+\cdot}$, 1342 [M]$^{+\cdot}$. UV−vis (CH_2Cl_2) λ_{max} nm (ϵ.10^{-3} M^{-1} cm^{-1}): 391 (280); 530 (14); 552 (14). IR (KBr) ν cm^{-1}: 3409 (OH), 2962, 2925, 2854 (CH); 1920 (CO).

Synthesis of H_2(DPA)[Ga(OH)] (4b) and (DPA)[Ga(OH)−Co(II)] (6). The hetero-bimetallic derivatives **4b** and **6** were prepared as already described.[7,30]

X-ray Crystallographic Experimental Data. X-ray diffraction data were collected with the following instruments: **2**, a Syntex $P2_1$ diffractometer with a modified Siemens LT-1 cooling device and a sealed tube [λ(Cu Kα) = 1.54178 Å (graphite monochromated)]; **5a**, a Nonius CAD4 with a Nonius cooling device and a sealed tube [λ(Mo Kα) = 0.71073 Å (graphite monochromated)]; **5b**, a Siemens R3m/V diffractometer equipped with a modified Nonius low-temperature apparatus and a sealed tube [λ(Mo Kα) = 0.71073 Å (graphite monochromated)]. The Bruker SHELXTL V. 5.03 software package was used for structure solution and refinement for **2** and **5b**; **5a** was solved by SHELXS and refined using SHELXL-97. Structures were refined (based on F^2 using all independent data) by full matrix least-squares methods. Illustrations of **2**, **5a**, and **5b** are shown in Figures 1−3. A short list of experimental details is given in Table 1. Additional experimental details, in CIF format, are available in the Supporting Information.

(15) Cox, G. S.; Whitten, D. G.; Giannotti, C. *Chem. Phys. Lett.* **1979**, *67*, 511.
(16) Richoux, M. C.; Neta, P.; Haniman, A.; Bard, S.; Hambright, P. *J. Phys. Chem.* **1986**, *90*, 2462−2468.
(17) Lindsey, J. S.; Delaney, J. K.; Mauzerall, D. C.; Linschitz, H. *J. Am. Chem. Soc.* **1988**, *110*, 3610−3621.
(18) Gentemann, S.; Albaneze, J.; Garcia-Ferrer, R.; Knapp, S.; Potenza, J. A.; Schugar, H. J.; Holten, D. *J. Am. Chem. Soc.* **1994**, *116*, 281−289.
(19) Walters, V. A.; de Paula, J. C.; Jackson, B.; Nutailis, C.; Hall, K.; Lind, J.; Cardozo, K.; Chandran, K.; Raitle, D.; Philips, C. M. *J. Phys. Chem.* **1995**, *99*, 1166−1171.
(20) Tait, C. D.; Holten, D.; Barley, M. H.; Dolphin, D.; James, B. R. *J. Am. Chem. Soc.* **1985**, *107*, 1930−1934.
(21) Antipas, A.; Dolphin, D.; Gouterman, M.; Johnson, E. C. *J. Am. Chem. Soc.* **1978**, *100*, 7705−7709.
(22) Slone, R. V.; Hupp, J. T. *Inorg. Chem.* **1997**, *36*, 5422−5423.
(23) Wagner, R. W.; Seth, J.; Yang, S. I.; Kim, D.; Bocian, D. F.; Hotten, D.; Lindsey, J. S. *J. Org. Chem.* **1998**, *63*, 5042−5049.
(24) Ohno, O.; Kaizu, Y.; Kobayashi, H. *J. Chem. Phys.* **1985**, *82*, 1779−1787.
(25) Ebeid, E. M.; Habib, A. M.; Abdel-Kader, M. H.; Yousef, A. B.; Guilard, R. *Spectrochim. Acta, Part A* **1988**, *44*, 127−130.
(26) Kim, K. Ph.D. Thesis, Stanford University, Stanford, CA, 1987.
(27) Eaton, S. S.; Eaton, G. R.; Chang, C. K. *J. Am. Chem. Soc.* **1985**, *107*, 3177−3184.
(28) Chang, C. K.; Abdalmuhdi, I. *J. Org. Chem.* **1983**, *48*, 5388−5390.
(29) Collman, J. P.; Garner, J. M. *J. Am. Chem. Soc.* **1990**, *112*, 166−173.
(30) Brandès, S. Thèse de l'Université de Bourgogne, Dijon, France, 1993.

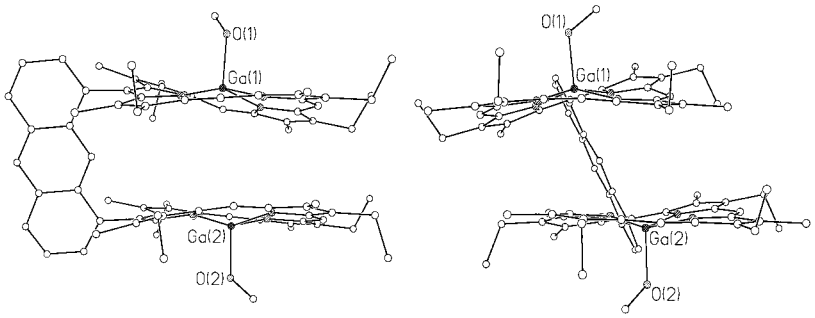

Figure 1. The molecular structure of (DPA)[Ga(OMe)]$_2$ (**2**) illustrating the cofacial nature of the porphyrin macrocycles and the axial methoxyl ligands bound on the unhindered porphyrin faces.

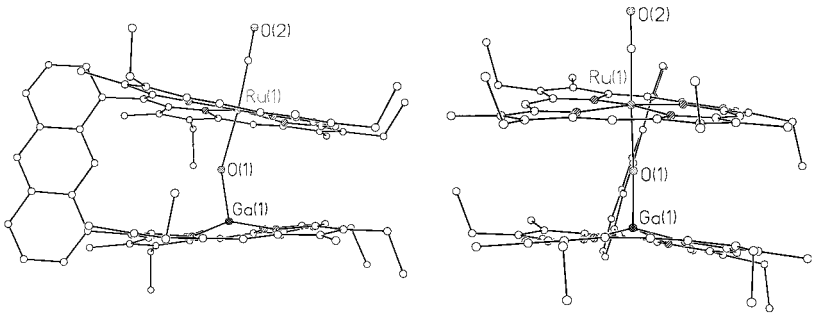

Figure 2. The molecular structure of (DPA)[Ga−(OH)−Ru(CO)] (**5a**); hydrogens have been omitted for clarity.

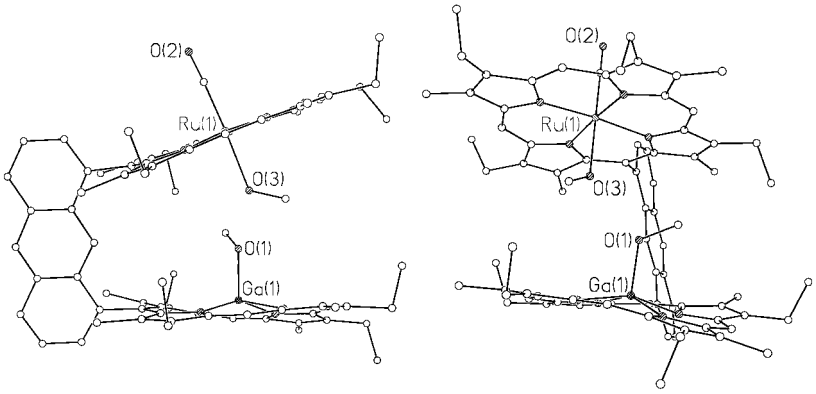

Figure 3. The molecular structure of (DPA)[Ga(OMe)−Ru(CO)(MeOH)] (**5b**); hydrogens have been omitted for clarity.

Instrumentation. The UV−vis spectra were recorded on a Varian Cary 1 spectrophotometer. Mass spectra were obtained with a Kratos Concept 32 S spectrometer in LSIMS mode (matrix: *m*-nitrobenzyl alcohol). Data were collected and processed using a Sun 3/80 workstation. The MALDI-TOF mass spectra were obtained on a Bruker Proflex III spectrometer in linear mode, with a nitrogen laser. The matrix was dithranol (1,8-dihydroxy-9[10H]-anthracenone). ^{1}H NMR spectra were recorded on a Bruker AMX 200 Fourier transform spectrometer at the Centre de Spectrométrie Moléculaire de l'Université de Bourgogne. All chemical shifts are given downfield from internal tetramethylsilane. NMR data are presented in the following order: chemical shift, peak multiplicity (br = broad, s = singlet, d = doublet, t = triplet, q = quartet, m = multiplet, dd = doublet of doublets), integration, and assignment. The luminescent spectra (excitation and emission) were acquired on a double-monochromator Fluorolog II instrument from Spex. All solutions were Ar-degassed prior measurements. The fluorescence lifetimes were measured using a single-photon-counting apparatus equipped with an N_2 flash lamp pulsing at 10 kHz. The full width at half-maximum was around 3.0 ns.

Procedure. The quantum yields were measured using 9,10-diphenylanthracene as standard ($\Phi_F = 1.0$). Due to the dichromophoric nature of the diporphyrins exhibiting excitation spectra that are function of the slightly different chromophores, Φ_F is function of λ_{exc}. Therefore, the reported Φ_F's were for $\lambda_{exc} = 392$ nm only and are used only to provide a qualitative relative estimate of the emission intensity.

Results and Discussion

Preparation and Characterization. The bis(gallium) porphyrin (DPA)[Ga(OMe)]$_2$ (**2**) is readily obtained in 80% yield by reacting the free base bis(porphyrins) (**1**) with an excess of $GaCl_3$ in benzonitrile according to Scheme 1. The synthesis of the monogallium derivative is not straightforward. Attempts to insert gallium into the free base H_4(DPA) (**1**) leads to a large amount of the bismetalated derivative due to the fact that, in the DPA series, the two porphyrins tend to behave as two independent macrocycles.[11] An alternative method has then been employed using zinc as protective agent on one of the two porphyrin macrorings (Scheme 1).[29] The good yield synthesis (77%) of the monozinc precursor H_2(DPA)Zn (**3**) has been previously reported.[11] After treatment with $GaCl_3$, the zinc−gallium intermediate species is reacted with HCl 6 M to give the monogallium derivative H_2(DPA)[Ga(OMe)] (**4a**) in a 32% yield (on the basis of H_4(DPA)). The heteronuclear complex (DPA)[Ga−(OH)−Ru(CO)] (**5a**) is then obtained by metalation of **4a** with $Ru_3(CO)_{12}$ in 35% yield.

All compounds have been fully characterized by means of ^{1}H NMR, IR, UV−vis spectroscopies, elemental analysis, and mass spectrometry.

Table 1. Selected Crystallographic Experimental Data for **2**, **5a**, and **5b**

	2	**5a**	**5b**
chemical formula	$C_{80}H_{84}Ga_2N_8O_2$, 3.8(CH_3OH)	$C_{79}H_{78}GaN_8O_2Ru$, 1.6(CH_2Cl_2)	2($C_{81}H_{85}GaN_8O_3Ru$) 0.53 THF 1.21 toluene 3.82 H_2O
formula weight	1452.81	1481.30	2949.33
space group	$P2_1$	$P2_1$	$P\bar{1}$
a (Å)	16.916(2)	21.011(3)	18.946(4)
b (Å)	19.428(3)	11.797(3)	21.535(4)
c (Å)	23.213(5)	30.347(4)	21.572(4)
α (deg)	90	90	18.946(4)
β (deg)	93.990(10)	110.725(12)	96.02(3)
γ (deg)	90	90	21.572(4)
Volume (Å^3)	7610(2)	7370(2)	8305(3)
Z	4	4	4
μ (mm^{-1})	1.321	2.941	0.554
total reflections	15593	13966	21055
unique reflections	10540	13966	21055
obsd reflections	6223 ($>2\sigma$(I))	8580($>2\sigma(I)$)	9811($>2\sigma(I)$)
$R(F_o^2)$ ($>2\sigma(I)$)[a]	0.096	0.102	0.100
$R_w(F_o^2)$ (all data)	0.275	0.293	0.317

[a] $R1 = \sum ||F_o| - |F_c|| / \sum |F_o|$ and $wR2 = [\sum[w(F_o^2 - F_c^2)^2] / \sum[w(F_o^2)^2]]^{1/2}$, $w = 1/[\sigma^2(F_o^2) + ((X)P)^2 + (Y)P]$ where $P = (F_o^2 + 2F_c^2)/3$ and for: (**2**), $X = 0.1370$ and $Y = 20.4902$; (**5a**), $X = 0.0200$ and $Y = 0$; (**5b**), $X = 0.1527$ and $Y = 6.7709$.

Scheme 1

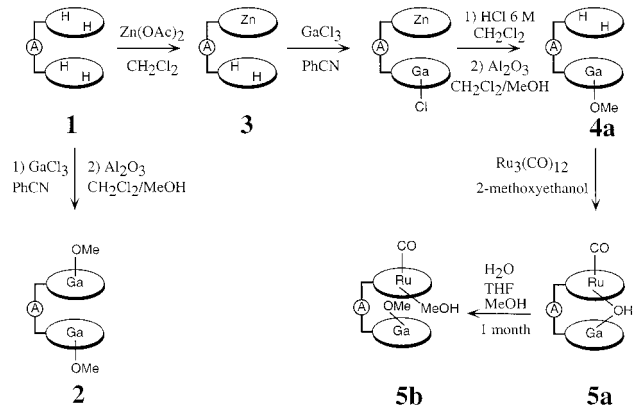

UV−vis data of the free base H_4(DPA) (**1**), the monogallium bis(porphyrins) H_2(DPA)[Ga(OMe)] (**4a**), the bis(gallium) bis(porphyrins) (DPA)[Ga(OMe)]$_2$ (**2**), the gallium−ruthenium bis(porphyrins) (DPA)[Ga−(OH)−Ru(CO)] (**5a**), and the gallium−cobalt bis(porphyrins) (DPA)[Ga(OH)−Co(II)] (**6**) are given in Table 2. Typically, the UV−vis spectrum of the free base H_4(DPA) exhibits an intense Soret signal around 400 nm and four *Q* bands, labeled I−IV, located between 500 and 700 nm. The optical density values of these four *Q* absorptions (IV > II > III > I) are characteristic of a so-called "phyllo" type spectrum.[31] Conveniently, the mono- and di-metalation reactions can be efficiently monitored by UV−vis spectroscopy. Indeed, going from the free base to the monometalated derivative leads to a decrease in intensity of the first and fourth Q-bands (at ∼ 500 and 630 nm) in comparison with the two centered ones. Upon dimetalation, disappearance of two bands at ∼630 and 500 nm, and intensity enhancement of the two middle bands at 539 and 578 nm occur. In addition, all the gallium derivatives exhibit a "regular" spectrum (for comparison purposes, the UV−vis data for (OEP)[Ga(OH)] and (TPP)[Ga(OH)] are also provided), while the spectrum of the gallium−ruthenium complex **5a** is of the "hypso" type.[31] In this case, the two bands at 530 and 552 nm undergo a large hypsochromic shift (9 and 26 nm respectively). Interestingly, "hypso" spectra have already been reported in the case of Ru(II) monoporphyrin. This hypsochromic shift can be explained by the destabilization of the levels $e_g(\pi^*)$ to higher energy due to a mixing of the filled $e_g(d_\pi)$ metal orbital (Ru: d^6) with the empty $e_g(\pi^*)$ orbitals of the porphyrinic ring (i.e., back-bonding).[32]

The IR data are given in the Experimental Section. The monometallic complexes exhibit NH vibrations at 3251 cm^{-1} for H_2(DPA)[Ga(OMe)] (**4a**), with a decrease in intensity, consistent with a loss of two protons. The IR spectrum of (DPA)[Ga−(OH)−Ru(CO)] (**5a**) exhibits a CO stretching absorption at 1920 cm^{-1}, characteristic of a terminal carbonyl group, and a ν(OH) vibration at 3409 cm^{-1}.[33]

The mass spectral data and the ^{1}H NMR data of the new homo- and heterobimetallic gallium derivatives are reported in the Experimental Section. No molecular peak is observed on the mass spectrum due to the relative lability of the gallium axial ligand(s) L. Therefore, the base peak is generally observed at $[M - L + NBA + 1]^+$, corresponding to the loss of the ligand L and interaction with the matrix (*m*-nitrobenzyl alcohol (NBA)). The ^{1}H NMR chemical shift spectral range of the gallium derivatives is characteristic of diamagnetic complexes (except for **6**). In the case of the bimetallic derivatives, the disappearance of the pyrrole NH resonance at high field unambiguously demonstrates the coordination of the two macrocycles. In the positive chemical shift region, no significant change is observed when the bis-gallium complex spectra and those of the starting free base macrocycles are compared.

Crystal Structures of (DPA)[GaOMe]$_2$ (2), (DPA)[Ga−(OH)−Ru(CO)] (5a), and (DPA)[Ga(OMe)−Ru(MeOH)-(CO)] (5b). The molecular structure of **2** is shown in Figure 1 and selected geometrical features are given in Tables 3 and 4. The Ga ions are pentacoordinated with axial methoxide ligands bound on the least encumbered faces of the porphyrin macrocycles. The metals are positioned 0.425(3) and 0.385(2) Å away from their respective PMPs (herein PMP, porphyrin mean plane, refers to the least-squares plane calculated for a porphyrin macrocycle's 24 carbon and nitrogen atoms). The location of

(31) Smith, K. M. In *Porphyrins and Metalloporphyrins*; Smith, K. M., Ed.; Elsevier Scientific: Amsterdam, 1975; Vol. I, p 3−28.

(32) Antipas, A.; Buchler, J. W.; Gouterman, M.; Smith, P. D. *J. Am. Chem. Soc.* **1978**, *100*, 3015−3024.

(33) Collman, J. P.; Kim, K.; Leidner, C. R. *Inorg. Chem.* **1987**, *26*, 1152−1157.

Table 2. UV−Vis Data for the H_4(DPA) Free Bases and the Gallium and Ruthenium Derivatives (rt, in methylene chloride except for **1** (rt, benzene))

	λ_{max}, nm (ϵ, 10^{-3} M^{-1} cm^{-1})				
compounds	Soret region		*Q* bands		
H_4(DPA) (**1**)	395 (190)	506 (14)	539 (5)	578 (6)	631 (3)
H_2(DPA)[Ga(OMe)] (**4a**)	394 (306)	507 (14)	541 (19)	579 (17)	628 (3)
H_2(DPA)[Ga(OH)] (**4b**)	394 (270)	506 (11)	540 (17)	576 (15)	628 (2.5)
(DPA)[Ga(OMe)]$_2$ (**2**)	393 (340)		535[a]/543 (16)	573 (13)/580[a]	640 (0.5)
(DPA)[Ga−(OH)−Ru(CO)] (**5a**)	391 (280)		530 (14)	552 (14)	578[a]/595s
(DPA)[Ga(OH)−Co(II)] (**6**)	394 (104)		542 (8)	570 (8)	
(OEP)[Ga(OH)]	395 (105)	494 (0.3)	533 (4)	571 (5)	629 (2.5)
(TPP)[Ga(OH)]	414 (250)	512 (2)	549 (9)	589 (3)	

[a] Shoulder.

Table 3. Crystallographically Determined Intradimer Geometrical Features for Anthracene (DPA), Biphenylene (DPB), and 1,2-diporphyrinyl Substituted Benzene Linked Cofacial Bisporphyrins

	Ct−Ct (Å)	M−M (Å)	M.P.S. (Å)	interplanar angle (deg)	slip angle (deg)	lateral shift (Å)	a−b distance	c−d distance
(DPA)[Ga(OMe)]$_2$ (**2**)	4.546(10)	5.247(2)	3.922(9)	7.2(2)	29.4	2.23	4.936(13)	4.887(12)
(DPA)[Ga(OMe)−Ru(MeOH) (CO)] (**5b**)	6.48(2)	6.172(3)	6.14(2)	22.6(2)	19.1	2.12	5.00(3)	5.18(2)
(DPA)[Ga−(OH)−Ru(CO)] (**5a**)	4.259(10)	3.9461(12)	4.232(10)	13.02(11)	7.6	0.56	4.946(14)	4.917(11)
(DPA)[Ni_2] [38]	4.56	4.57	3.87	2.4	31.7	2.40	4.961	4.927
(DPA)[Lu(OH)]$_2$·CH_3OH [39]	5.638	3.523	5.689	19.7	10.5	1.02	4.930	4.973
(DPA′)[Fe_2(μ−im)(Him)$_2$]·Cl [40]	5.96	5.96	5.78	28.4	14.2	1.46	4.995	5.027
(DPB)[Cu_2] [36]	3.862	3.807	3.522	4.4	25.0	1.63	3.797	3.802
(DPB)[CuMn]·Cl [11]	3.916	4.126	3.562	5.2	25.7	1.70	3.770	3.814
(DPB)[Lu(OH)]$_2$·CH_3OH [39]	5.542	3.526	5.509	27.1	13.9	1.33	3.849	4.176
(DPB)[Co−Al(OEt)] [10]	4.083	4.37	3.558	7.4	29.8	2.03	3.778	3.821
(DPB)[Co_2] [1]	3.769	3.727	3.471	4.3	23.8	1.52	3.785	3.778
(1,2-DPBenzene)[Zn_2] [47]	3.942	3.853	3.467	6.5	29.1	1.92	1.391	2.814

Table 4. Selected Bond Lengths and Geometrical Features for **2**, **5a**, and **5b**[a]

	2	**5a**	**5b**
Ga1−N1	2.016(8)	2.050(7)	2.042(9)
Ga1−N2	2.025(10)	2.052(7)	2.051(11)
Ga1−N3	2.022(7)	2.016(6)	2.051(9)
Ga1−N4	2.026(8)	2.050(7)	2.025(10)
Ga2/Ru1−N5	2.039(7)	2.055(6)	2.079(9)
Ga2/Ru1−N6	2.025(6)	2.068(7)	2.066(10)
Ga2/Ru1−N7	2.029(7)	2.056(6)	2.075(10)
Ga2/Ru1−N8	2.050(7)	2.062(6)	2.052(9)
Ga1−O1	1.856(6)	1.852(5)	1.850(8)
Ga2−O2 or Ru1−O1/O3	1.861(5)	2.183(5)	2.212(9)
Ru1−C		1.784(8)	1.82(2)
Ga1−PMP dist	0.425(3)	0.455(2)	0.442(3)
Ga2/Ru1−PMP dist	0.385(2)	0.117(2)	0.093(3)
Ga1 macro MDPMP	0.242	0.113	0.157
Ga2/Ru1 macro MDPMP	0.146	0.082	0.048

[a] In **5b**, data are for molecule #1. Data for molecule #2 are available in the Supporting Information.

the Ga ions results in a metal-to-metal distance of 5.247(2) Å while the DPA ligand maintains a smaller center-to-center distance of 4.546(10) Å (see Figure 4 for geometrical measurement definitions). Both porphyrin macrocycles are slightly nonplanar with a mixture of sad/ruf nonplanar distortions[34] and exhibit MDPMPs[35] of 0.242 and 0.146 Å. Aside from the methoxide ligands and the positioning of the metal ions the DPA ligand of **2** is notably similar (as reflected in Table 3) to that reported for DPA[Ni_2].[36]

The molecular structures of **5a** and **5b** are shown in Figures 2 and 3, respectively; selected geometrical features are given in Tables 3 and 4. In **5b**, the Ga ion is pentacoordinated, with an axial methoxide ligand, and positioned 0.442(3) Å above its PMP as shown in Figure 3 (there are two nearly isostructural molecules in the asymmetric unit, measurements are given for one molecule, called molecule #1). The Ru metal atom is hexacoordinated and sitting nearly in its PMP. The latter is bonded to an axial carbonyl ligand located on the least hindered porphyrin face, and to an axial methanol molecule, which lies between the two porphyrin macrocycles. The center-to-center distance is 6.48(2) Å while the metal-to-metal distance is 6.172(3) Å. Intramolecular repulsive forces between the porphyrin macrocycles are illustrated by a close contact between the internal axial methoxyl and methanol ligands [O to O distance: 2.666(12) Å]. These repulsions result in the largest mean plane separation, center-to-center, metal-to-metal, and c−d distances (Figure 5) thus far observed for any of the available crystal structures[37] from the DPA/DPB series (Table 4). The Ga bearing macrocycle exhibits a MDPMP of 0.157 Å with a sad/ruf nonplanar conformation.[34] The Ru bearing macrocycle of **5b** is nearly planar with a MDPMP[35] of 0.048 Å.

Compound **5a** exhibits the same metals and porphyrinic ligand as **5b** but is notably different in that it demonstrates an intramolecular Ga−OH−Ru bridge with the hydroxyl anion held between the two porphyrin macrocycles as shown in Figure 2. The Ga ion is pentacoordinated and positioned 0.455(2) Å above its PMP and between the two porphyrin macrocycles. The Ru ion is hexacoordinated, with an axial carbonyl group on its unhindered porphyrin face, and resides nearly in its PMP. The result of the bridging hydroxyl ligand is that **5a**, in contrast to **5b**, exhibits the smallest center-to-center distance (4.259(10) Å), slip angle, and lateral shift of any of the DPA series (Table

(34) Jentzen, W.; Song, X. Z.; Shelnutt, J. A. *J. Phys. Chem.* **1997**, *B101*, 1684.
(35) MDPMP: the mean deviation of the 24 porphyrin macrocyclic atoms from their least-squares plane (metal ions are not included in this calculation).
(36) Fillers, J. P.; Ravichandran, K. G.; Abdalmuhdi, I.; Tulinsky, A.; Chang, C. K. *J. Am. Chem. Soc.* **1986**, *108*, 417−424.
(37) Available crystal structures refer to those contained within The Cambridge Structural Database, April 2000 release, provided by the Cambridge Cristallographic Data Center.

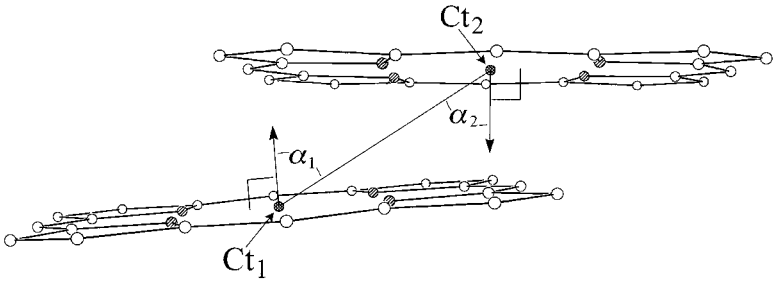

Figure 4. Illustration of the method by which the selected crystallographically derived geometrical features were measured. Macrocyclic centers (Ct) were calculated as the centers of the 4-N planes for each macrocycle. The interplanar angles were measured as the angle between the two macrocyclic 24-atom least-squares planes. Plane separations were measured as the perpendicular distance from one macrocycle's 24 atom least-squares plane to the center of the other macrocycle; reported mean plane separations (M. P. S.) were the average of the two plane separations for each dimer. The slip angles (α) were calculated as the average angle between the vector joining the two macrocyclic centers and the unit vectors normal to the two macrocyclic 24-atoms least-squares planes (α = $\alpha_1 + \alpha_2/2$). Lateral shift was defined as [sin(α) × (Ct−Ct distance)].[10 42 49]

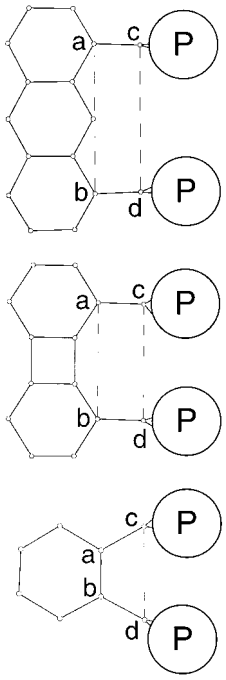

Figure 5. A series of aromatic linking units used to join porphyrin monomers to form the cofacial porphyrin dimers DPA (top: 1,8-diporphyrinylanthracene, P = porphyrinyl), DPB (middle: 1,8-diporphyrinylbiphenylene), and 1,2-diporphyrinylbenzene (bottom). The illustrated distances (a−b and c−d) are given in Table 3 for all reported crystal structures of these types.

3). The metal-to-metal distance in **5a** is 3.9461(12) Å. The structures of **5a** and **5b** demonstrate the ability of the DPA ligand to open and close its "bite" around the binding pocket as described by Collman et al.[38] The Ga bearing macrocycle is slightly nonplanar with a MDPMP[35] of 0.113 Å (sad/ruf mixture),[34] while the Ru bearing macrocycle displays a MDPMP of 0.082 Å (sad/wav mixture).[34] There are other examples of crystal structures in the DPA/DPB series which bear internal metal-bridging axial ligands. In the (DPA)[Lu(OH)]$_2$·CH_3OH and (DPB)[Lu(OH)]$_2$·CH_3OH structures[39] the pairs of Lu ions are also bridged via hydroxyl anions. Additionally, in the [(DPA′)Fe_2(μ-im)(Him)$_2$]Cl structure,[40] an imidazole moiety bridges the molecule's two Fe centers.

Chart 1

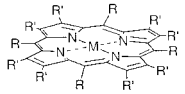

Free-base monoporphyrins
H_2(TPP): R = Ph; R′ = H; M = 2H
H_2(OEP): R = H; R′ =Et; M = 2H

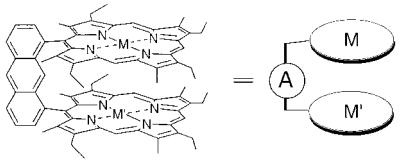

H_4(DPA) : Ar = Anthracene bridge

(**1**) : M = M′ = 2H
(**2**) : M = M′ = Ga(OMe)
(**3**) : M = Zn, M′ = 2H
(**4a**) : M = 2H, M′ = Ga(OMe)
(**4b**): M = 2H, M′ = Ga(OH)
(**5a**) : M = Ru(CO), M′ = Ga-(OH)-
(**5b**): M = Ru(CO)(MeOH), M′ = Ga(OMe)
(**6**) : M = Co(II), M′ = Ga(OH)

The three new crystal structures reported herein, along with the other nine previously reported structures from the DPA, DPB, and 1,2 diporphyrinylbenzene series (as enumerated in Table 3 and Figure 5), represent a growing body of structural data on rigidly linked cofacial porphyrin dimers (recent reports of xanthene- and dibenzofuran-bridged cofacial bisporphyrins are not discussed herein[41]). With the results accumulated thus far it should be possible to fine-tune these ligands to afford desired structural features within a significant range for several of the salient parameters. The center-to-center distances can be partially regulated via choice of the appropriate linking unit such as anthracene, biphenylene, or benzene. In the absence of internal axial ligands the center-to-center distances are ∼4.5 Å for the DPAs and ∼3.9 Å for the DPB and 1,2 diporphyrinylbenzene compounds. Another structural aspect of these molecules which can be influenced by the choice of linking unit relates to the degree of intramolecular $\pi-\pi$ stacking between the porphyrin macrocycles. For porphyrins, these effects are considered to be strong when mean plane separations are ∼3.3−3.5 Å combined with lateral shifts of ∼1.2−2.1 Å.[42] Among the DPAs, which have a−b distances (Figure 5) of ∼4.95 Å, $\pi-\pi$ stacking appears to be weak in the cases of the di-Ni and

(38) Collman, J. P.; Wagenknecht, P. S.; Hutchison, J. E. *Angew. Chem., Int. Ed. Engl.* **1994**, *33*, 1537−1554.
(39) Lachkar, M.; Tabard, A.; Brandès, S.; Guilard, R.; Atmani, A.; De Cian, A.; Fischer, J.; Weiss, R. *Inorg. Chem.* **1997**, *36*, 4141−4146.
(40) Naruta, Y.; Sawada, N.; Tadokoro, M. *Chem. Lett.* **1994**, 1713−1716.
(41) Deng, Y.; Chang, C. J.; Nocera, D. J. *Inorg. Chem.* **2000**, *39*, 959.
(42) Scheidt, W. R.; Lee, Y. J. *Struct. Bonding (Berlin)* **1987**, *64*, 30−31.

di-Ga species and nonexistent for those with internal axial ligands. For the DPBs, which have a−b distances of ∼3.80 Å, $\pi-\pi$ stacking is stronger but it too can be alleviated by the presence of internal axial ligands. The metal-to-metal distances can be regulated by a number of structural features; foremost among these would be the center-to-center distances and the influence of axial ligands. A notable example of this is the structure of **2** (Figure 1); therein, while the center-to-center distance was 4.546(10) Å, the metal-to-metal distance was 5.247(2) Å. This feature was a result of the positioning of the Ga ions away from the PMPs on the unencumbered faces of the porphyrin macrocycles. A corollary to this is the structure of **5a** in which the Ga ion was again positioned away from the PMP, but in this case closer to the 4-N center of the opposing macrocycle. Slip angles, lateral shifts, and interplanar separations could be regulated by the presence of bridging and nonbridging axial ligands as illustrated by the structures of **5a** and **5b** (Figures 2 and 3). A wide variety of internal axial ligands or direct metal−metal bonds could force the porphyrin macrocycles to span even greater distances or become more tightly held together.

Luminescence Study. These bichromophoric systems are expected to reveal complex multiluminescence behavior. The porphyrin chromophore is known for $S_2 \rightarrow S_0$ and $S_1 \rightarrow S_0$ fluorescence, as well as $T_1 \rightarrow S_0$ phosphorescence, as detected for many metalloporphyrins.[19,24,43] Although weak emissions attributable to $S_2 \rightarrow S_0$ fluorescence has been detected in the 400−600 nm region for these cofacial diporphyrins, these luminescences have not been analyzed in this work.

The H_4(DPA) (**1**) used as model compound exhibits a strong but modestly vibrationnally structured luminescence band between 620 and 800 nm ($\Phi = 0.020$) at 298 K. At 77 K, the luminescence band becomes more intense ($\Phi = 0.044$) and clearly more structured (Supporting Information). The luminescence decay in the ns time scale (10.2 ns (298 K) and 24.0 ns (77 K)) and the very small Stokes shift for the 0−0 transitions (620 and 622.5 nm; ∼65 cm^{-1}) clearly indicate fluorescence. These spectroscopic and photophysical data present a clear signature of the fluorescent $^1\pi\pi^*$ state of the porphyrin fragment and compare favorably to that of porphyrin itself (H_2P; $\Phi_F = 0.054$, $\tau_F = 15.3$ ns, in benzene at room temperature).[24] The smaller Φ_F and τ_F values in the diporphyrin species are very likely due to vibrations and intramolecular collisions promoting excited-state deactivation.

Prior discussion of the luminescence properties of (DPA)[Ga(OMe)]$_2$ (**2**), the bichromophoric nature of the metallomonoporphyrin itself must be addressed. The absorption spectra of (TPP)[Ga(OH)] and (OEP)[Ga(OH)] are investigated (Supporting Information) and exhibit maxima (CH_2Cl_2) λ_{max} nm (ϵ 10^{-3}.M^{-1} cm^{-1}) at 396 (20.8), 414 (249.7), 512 (2.0), 549 (9.0), 589 (3.3), and 629 nm (2.5) and at 376 (10.1), 395 (105), 494 (0.3), 533 (3.7), and 571 nm (5.1), respectively, in ethanol at 298 K. A dilute solution containing 1:1 (TPP)[Ga(OH)] and (OEP)[Ga(OH)] generates a spectrum that is the sum of the individual spectra and compares very favorably to that of (DPA)[Ga(OMe)]$_2$ (**2**) (Supporting Information), with the difference of very minor shifts. This experiment indicates that some bands are associated or affected by the presence of an aryl group in position 5 (lower energy), and others with the alkyl groups in positions 2, 3, 7, 8, 12, 13, 17, and 18 (higher energy), in (DPA)[Ga(OMe)]$_2$ (**2**).

The latter (DPA)[Ga(OMe)]$_2$ (**2**) exhibits a double emission at both temperatures in the 500−800 nm region, where two 0−0 origins are readily depicted on the absorption (600 and 572 nm; 298 K) and emission spectra (580 and 620 nm; 298 K) (Figure 6). In both cases the excitation spectra match the absorption spectrum, with the obvious exception that the 600 nm peak does not appear in the spectra monitored at 580 nm. These results illustrate that these are the same chromophores. The ns time scale observed for τ_e (Table 5) indicates that the luminescences are fluorescence in both cases (measured at both extremeties of the spectra to avoid interference; 580 and 730 nm). At 77 K, the double emission behavior remains as stated, precluding the possibility of hot bands. Some improvement in vibrational resolution is also observed. The reported τ_F data for (TPP)[Ga(X)] and (OEP)[Ga(X)] species vary from ∼1 ns to 5.5 ns depending on the solvent and X (X = Cl, Br, OH),[24] and compare favorably to that of Ga species in this work. We assign the "blue" and "red" fluorescences to the singlet "octaalkylporphyrin" and "arylporphyrin" $\pi\pi^*$ states, respectively, and they will be referred as fluorescence I and fluorescence II. To our knowledge, this double fluorescence arising from Q-bands is unprecedented.[44] The reason the higher energy fluorescence I is not efficiently quenched by an anticipated energy transfer to the lower energy $\pi\pi^*$ state is unknown. This result urged us to investigate heterobiporphyrin systems in an attempt to see whether this behavior is specific to di-Ga.

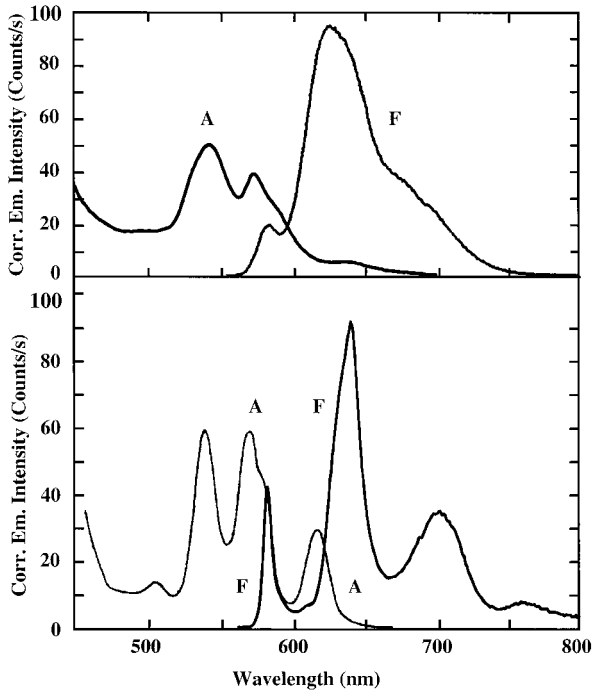

Figure 6. Absorption and fluorescence spectra of (DPA)[Ga(OMe)]$_2$ (**2**) in ethanol at 298 K (up) and 77 K (down). $\lambda_{exc} = 407$ nm.

The H_2(DPA)[Ga(OMe)] (**4a**) and H_2(DPA)[Ga(OH)] (**4b**) luminescence spectra are dominated by the H_2(DPA) $\pi\pi^*$ fluorescence, where Φ_F (H_2(DPA)) is about 2.5 order of magnitude greater than Φ_F ((DPA)[Ga(OR)]) (R = H, Me) at both temperatures. The emission bands associated with the

(43) Aaviksoo, J.; Freiberg, A.; Savikhin, S.; Stelmakh, G. F.; Tsvirko, M. P. *Chem. Phys. Lett.* **1984**, *111*, 275−278.

(44) To address the role of the molecular structure on this double emission, the emission and excitation spectra of the closely related monogallium porphyrin (gallium chloride 2, 8, 13, 17-tetraethyl-3, 7, 12, 18-tetramethyl-5-phenylporphyrinate) at room temperature in THF, have been examined. The structured emission spectrum exhibits maxima of vibronic origins at 588 and 635 nm, and the excitation spectrum superposes the absorption. There is no evidence for double emission for this compound. The preparation and characterization of this compound, along with the fluorescence and excitation spectra can be found in the Supporting Information.

Table 5. Photophysical Data for the Dimetalloporphyrins[a]

compound	lumophore	298K	77 K
H_4(DPA) (**1**)	H_4(DPA)	$\tau_F = 14.15$ ns $\Phi_F = 0.020$	$\tau_F = 24.0$ ns $\Phi_F = 0.044$
(DPA)[Ga(OMe)]$_2$ (**2**)	(DPA)[Ga(OMe)]	$\tau_F = 3.5$ ns $\Phi_F = 0.00075$ $\tau'_F = 4.4$ ns $\Phi'_F = 0.0039$	$\tau_F = 5.20$ ns $\Phi_F = 0.0055$ $\tau'_F = 5.1$ ns $\Phi'_F = 0.0065$
H_2(DPA)[Ga(OMe)] (**4a**)	H_2(DPA)	$\tau_F = 11.0$ ns $\Phi_F = 0.012$	$\tau_F = 24.0$ ns $\Phi_F = 0.020$
	(DPA)[Ga(OMe)]	$\tau_F = ?$[b] $\Phi_F = 0.00085$[c]	$\tau_F = 3.21$ $\Phi_F = 0.00086$[c]
H_2(DPA)[Ga(OH)] (**4b**)	H_2(DPA)	$\tau_F = 10.9$ ns $\Phi_F = 0.010$	$\tau_F = 24.9$ ns $\Phi_F = 0.019$
	(DPA)[Ga(OH)]	$\tau_F = ?$[b] $\Phi_F = 0.00051$[c]	$\tau_F = 5.5$ ns $\Phi_F = 0.00087$[c]
(DPA)[Ga(OH)−Co(II)] (**6**)	(DPA)[Ga(OH)]	$\tau_{F = 4.4\ ns}$ $\Phi_{F = 0.00059}$	$\tau_{F = 5.1\ ns}$ $\Phi_{F = 0.00081}$
(DPA)[Ga−(OH)−Ru(CO)] (**5a**)	(DPA)[Ga(OMe)]	$\tau_F = 4.5$ ns $\Phi_F = 0.00095$	$\tau_F = 3.3$ ns $\tau_P = 650$ ns $\Phi_F = 0.00102$ $\Phi_P = 0.00203$

[a] In EtOH. The uncertainty on τ_F is ±0.3 ns and on $\Phi_{F,P}$ (λ_{exc} = 392 nm) is ±10%, based upon multiple measurements on different samples. [b] Strong spectral overlaps occur with the free base luminescence, and the weakness of the intensity in this case precludes observation or deconvolution of the τ_F data associated to the GaOL−porphyrin fluorescence (L = H, Me). [c] Since the fluorescence band with the 0−0 peak at ∼580 nm is partially obscured by the more intense free base fluorescence, the area under the emission band has been estimated using the (DPA)[Ga−(OH)−Ru(CO)] (**5a**) and (DPA)[Ga(OH)−Co(II)] (**6**) fluorescences as references.

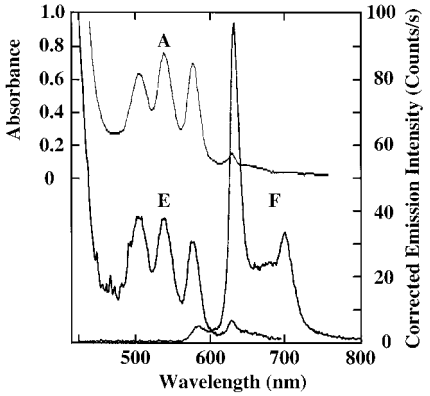

Figure 7. Absorption, excitation (λ_{emi} = 710 nm), and fluorescence (λ_{exc} = 410 nm) of H_2(DPA)[Ga(OH)] (**4b**) in ethanol at 298 K.

(DPA)[Ga(OR)] fragment exhibit a 0−0 peak at ∼581 nm, corresponding to the absorption peak at 578 nm (Figure 7). The ns time scale for τ_e (5.5 (R = H) and 3.9 ns (R = Me) at 77 K) and the position of the 0−0 peak allow to assign this luminescence to fluorescence I discussed above. The Φ_F data for the H_2(DPA) fragment is ∼ half of that of H_4(DPA). This is no surprise due to the bichromophoric nature of these species. The strong overlap between the two fluorescence bands preclude observation of the "complete" H_2(DPA)[Ga(OR)] spectra (i.e. fluorescences I and II). In fact, there is no evidence that confirms or contradicts the presence of fluorescence II. In the (DPA)-[Ga(OH)−Co(II)] (**6**) and (DPA)[Ga−(OH)−Ru(CO)] (**5a**) species, the transition metallomonoporphyrin fragments are not luminescent and the (DPA)[Ga(OR)] fluorescence is cleared from interference. In these cases the H_2(DPA)[Ga(OR)] fluorescence I signature is demonstrated by comparison of position of the 0−0 peak (Figure 8) and τ_F at both temperatures with the above species (Table 5). The absence (or extreme weakness) of luminescence for the Co(II) fragment is not surprising. This phenomenum is well documented in the literature for both Co(II) and Co(III) monoporphyrin derivatives.[45−47] Gouterman and

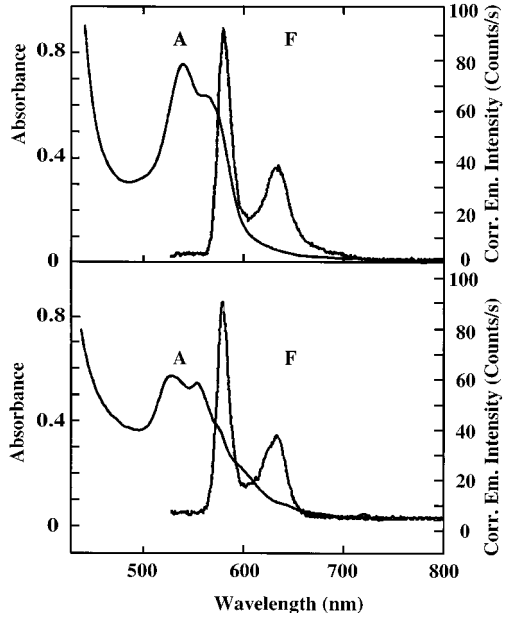

Figure 8. Absorption and fluorescence (λ_{exc} = 510 nm) of (DPA)-[Ga(OH)−Co(II)] (**6**) (up) and (DPA)[Ga−(OH)−Ru(CO)] (**5a**) (down) in ethanol at 298 K.

Antipas[45] explained that these emissions are quenched by lower energy forbidden (π,d) or (d,d) states.[24,45−47] The associated weak $\pi \rightarrow$d and d$\rightarrow$d absorptions were indeed observed in the near-IR spectra (700 < λ < 1100 nm) for (OEP)[Co(II)] and (TPP)[Co(II)] in CH_2Cl_2 at room temperature (75 < ϵ < 120 $M^{-1}cm^{-1}$).[45] Low intensity absorptions are also detected in this same region for (DPA)[Ga(OH)−Co(II)] (**6**) (Supporting Information). The absence (or extreme weakness) of luminescence for the porphyrin [(Ru(II))(CO)(OH)] fragment, at least at 298 K in deoxygenated solutions, is also consistent with similar

(45) Antipas, A.; Gouterman, M. *J. Am. Chem. Soc.* **1983**, *105*, 4896−4901.
(46) Ake, R. L.; Gouterman, M. *Theor. Chim. Acta* **1969**, *15*, 20−42.
(47) Eastwood, D.; Gouterman, M. *J. Mol. Spec.* **1970**, *35*, 359−375.
(48) Osuka, A.; Nakajima, S.; Nagata, T.; Maruyama, K.; Toriumi, K. *Angew. Chem., Int. Ed. Engl.* **1991**, *30*, 582.
(49) Clement, T. E.; Nurco, D. J.; Smith, K. M. *Inorg. Chem.* **1998**, *37*, 1150−1160.

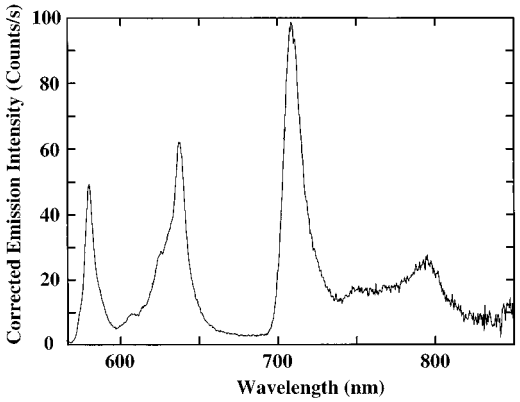

Figure 9. Emission spectrum of (DPA)[Ga−(OH)−Ru(CO)] (**5a**) (down) in ethanol at 77 K.

literature findings.[20] A state responsible for a weak absorption at 710 nm, presumably (π, d), is invoked to be at the origin of this quenching.[20] A shoulder at $\sim$ 750 nm ($\epsilon \sim 90$ $M^{-1}cm^{-1}$) is indeed expectedly observed in the (DPA)[Ga−(OH)−Ru-(CO)] (**5a**) near-IR spectra (Supporting Information). At 77 K, a new emission is readily detected between 700 and 800 nm (Figure 9), with a 0−0 transition at 709 nm. The lowest energy absorption band is located at 777 nm at 298 K (CH_2Cl_2; saturated solution), and the relatively long τ_e (650 ns in 2-MeTHF at 77 K) demonstrates that this luminescence is phosphorescence. The nature of the phosphorescence is unambiguously established from the comparison with the (OEP)[Ga-(Cl)] phosphorescence spectrum, which is practically identical.[24] The only difference is that τ_p is much longer in the later case (140 ms). The (TPP)[Ga(Cl)] phosphorescence spectrum exhibits a strong and narrow peak at $\sim$758 nm, but no such band is observed for both (DPA)[Ga(OL)-M′] species. It appears clear that the lowest energy singlet states, which give rise to fluorescence II (and triplet states as well), are all efficiently quenched by Co(II) and Ru(II) centers. These findings are consistent with literature and further demonstrate the presence of intermolecular energy transfer. It is surprising that the higher energy fluorescence I is not quenched as efficiently, based on the τ_F data.

Conclusion. A new series of heterobimetallic cofacial diporphyrins has been prepared containing the luminescent Lewis acid porphyrin GaOL center. Interactions with substrates such as dioxygen should be spectroscopically and photophysically sensored, hence providing some information on the intermediate species responsible for dioxygen reduction by cofacial cobalt(II) diporphyrins. The effect of dioxygen on the emission and photophysical properties of cofacial (DPA)$[Ga(OL)]_2$, (DPA)-[Ga(OL)−Co(II)], (DPA)[Ga(OL)−Co(III)], and (DPA)$[Co(II)]_2$ species will be reported in due course. In addition the presence of multiple fluorescence in (DPA)$[Ga(OMe)]_2$ (**2**) deserves attention of a theoretical and spectroscopic stand point. Careful examination of the luminescence behavior as a function of substitution on Ga-monoporphyrins and the effect of the spacer on these parameters is clearly required.

Acknowledgment. P. D. H. thanks NSERC (Natural Sciences and Engineering Research Council of Canada) and FCAR (Fonds Concertés pour l'Avancement de la Recherche) for support. K. M. S. thanks the USA National Science Foundation (NSF CHE-99-04076) for support. We would also like to acknowledge Dr. R. G. Khoury for collecting the data sets and performing the structure solution for the X-ray crystal structure determinations of **2** and **5b**. The support of the CNRS (R.G., UMR 5633) is also gratefully acknowledged. Marcel Soustelle (L.I.M.S.A.G.) is acknowledged for synthetic contributions.

Supporting Information Available: Excitation and fluorescence spectra of H_4(DPA) (**1**) (Figure S10); comparison of the absorption spectra of (TTP)[Ga(OH)] and (OEP)[Ga(OH)] (Figure S11) and 1:1 (OEP)[Ga(OH)]/(TPP)[Ga(OH)] and (DPA)$[Ga(OMe)]_2$ (**2**) (Figure S12); near-IR spectra of (DPA)[Ga(OH)−Co(II)] (**6**) and (DPA)[Ga−(OH)−Ru(CO)] (**5a**) (Figure S13); fluorescence and excitation spectra of gallium chloride 2,8,13,17-tetraethyl-3,7,12,18-tetramethyl-5-phenylporphyrinate (Figure S14); and preparation and characterization data for gallium chloride 2,8,13,17-tetraethyl-3,7,12,18-tetramethyl-5-phenylporphyrinate. X-ray crystallographic files are available for **2**, **5a**·1,6-(CH_2Cl_2), **5a**·2(THF), and **5b** in CIF format. This material is available free of charge via the Internet at http://pubs.acs.org.

IC001446J